Security-Constrained Unit Commitment with Linearized System Frequency Limit Constraints

Hamed Ahmadi, *Student Member, IEEE,* and Hassan Ghasemi, *Senior Member, IEEE*

***Abstract*—Rapidly increasing penetration level of renewable energies has imposed new challenges to the operation of power systems. Inability or inadequacy of these resources in providing inertial and primary frequency responses is one of the important challenges. In this paper, this issue is addressed within the framework of security-constrained unit commitment (SCUC) by adding new constraints representing the system frequency response. A modified system frequency response model is first derived and used to find analytical representation of system minimum frequency in thermal-dominant multi-machine systems. Then, an effective piecewise linearization (PWL) technique is employed to linearize the nonlinear function representing the minimum system frequency, facilitating its integration in the SCUC problem. The problem is formulated as a mixed-integer linear programming (MILP) problem which is solved efficiently by available commercial solvers. The results indicate that the proposed method can be utilized to integrate renewable resources into power systems without violating system frequency limits.**

***Index Terms*—Security-constrained unit commitment, inertial response, primary frequency control, wind power.**

NOMENCLATURE

$\bar{B}$	Network susceptance matrix.
$\bar{D}$	Matrix product of the susceptance and node-incident matrices.
D	Load damping factor.
b	Generator's bid.
C^{SDn}	Shutdown cost.
C^{SUp}	Startup cost.
C_T	System total cost.
ΔP_d	Power imbalance disturbance.
F	Power fraction from HP turbine.
f^0	System nominal frequency.
$f^{\min}$	System minimum frequency.
$H(=0.5M)$	Generator inertia.
K	Mechanical power gain factor.
Ω	Large positive constant.
N_b, N_g	Sets of buses and generators, respectively.
N_l, N_t	Sets of lines and time horizon, respectively.
P	Generator active power.
$P^{\max}$, $P^{\min}$	Upper/lower limits on generator active power.
P_d	Active power demand.
P_i^L	Active power flow limit of Line i.
P^{SDn}	Generator minimum power limit at shutdown.
P^{SUp}	Generator maximum power limit at startup.
R^{Dn}	Generator power ramp-down limit.
R^{Up}	Generator power ramp-up limit.
R	Governor droop.
S	Set of PWL partitions.
SDn, SUp	Auxiliary variables for shutdown/startup cost.
T	Governor reheat time constant.
$T^{\text{Up}}, T^{\text{Dn}}$	Generator minimum up/down time.
$T_0^{\text{Up}}, T_0^{\text{Dn}}$	Generator initial up/down time.
u	Generator status (0:'Off', 1:'On').
v	Auxiliary binary variable for PWL.
δ	Bus voltage angle.
$\Delta\omega$	Frequency deviation.

H. Ahmadi is with the School of Electrical and Computer Engineering, University of British Columbia, Vancouver, BC, Canada, V6T 1Z4. E-mail: hameda@ece.ubc.ca. H. Ghasemi is with the School of Electrical and Computer Engineering, University of Tehran, Tehran, Iran, P. O. Box: 11365-4563. E-mail: h.ghasemi@ut.ac.ir.

I. INTRODUCTION

FOLLOWING an unexpected disturbance causing a mismatch between power supply and demand within a power system, the system frequency starts deviating from the nominal value. In a real system, frequency drop caused by loss of generation or frequency jump caused by loss of load are of crucial importance. Solving the time-domain equations describing power system dynamics would lead to different rotational speed for each generator during the transient period. For this reason, using the speed of a specific generator to represent system overall frequency condition is controversial. There have been many efforts to find the system average frequency trajectory and avoiding the computationally expensive time-domain solutions, e.g. [1] and [2]. In these studies, an important assumption is made, which is to have a unique frequency variation throughout the system.

Rapidly increasing penetration of renewable energies into the power systems has made the system operators encounter new challenges in terms of maintaining power system security. In particular, wind power, as the leading source of renewables, has introduced many operational issues at high penetration levels. In the United States, the Federal Energy Regulatory Commission (FERC) has announced a new study that analyzes system frequency response to evaluate the security of integration of renewables [3]. The Electric Reliability Council of Texas (ERCOT) has also shown concerns about installing new wind generations and possible drawbacks for system frequency response [4]. An approximation method is also proposed in [4] for the system operator to be aware of system inertial response in online operation. It is shown that the increased level of wind parks in the British system has led to acquiring higher system primary reserve [5]. In [6], it is shown, within a long-term study, that the wind generation penetration would deteriorate the system inertial and primary frequency responses. Similar concerns about system dynamic stability and frequency response have been reported in Iowa [7], Crete

(Greece) [8] and Ireland [9].

The problem arisen from integrating large amount of wind generation originates from the inability of widely used variable speed wind turbine technologies in providing inertial response and participation in frequency regulation in a similar way as the conventional synchronous generators. Recently, the problem of reduced inertia of wind turbines which use the doubly-fed induction generators or permanent magnet synchronous generators technologies has been addressed in some prototypes. Advanced control methods in active power modulation can inject more active power during sudden frequency drops by releasing the kinetic energy stored in the turbine shaft [10]. However, this sudden energy release would reduce the rotor speed almost immediately. The resulted extreme mechanical stress imposed on the shaft and drive train would lead to higher manufacturing cost of mechanical parts [11]. In addition, the wind generations are almost unable to provide primary/secondary frequency control during contingencies due to lack of operational reserve. In fact, it would be uneconomic to always use a portion of the whole available power from wind farms just to have some operational reserve. Besides, the probabilistic nature of wind speed makes the results of deterministic studies less reliable [12]. A few solutions for this problem are available in the literature and are reviewed in the next paragraph.

The problem of ensuring frequency response within an electricity market is studied in [13]. Two constraints are added to the problem of economic dispatch: one for limiting the rate of change of frequency and the other one for limiting the maximum frequency drop. However, the impact of each individual generator governor response cannot be seen in these constraints. Also, the off-line calculation of the second constraint may need to be done again if the system parameters change. The power flow and generators constraints are also left behind in [13]. These issues are addressed in the present study.

The system frequency deviation after a contingency can be approximately derived based on static analysis. Inertial and governor load flow are the well-known static analysis of system frequency response [14]. A first order model for system frequency response considering the governor droops has also been used in [15]. The differential equations are then discretized using integration rules to derive linear equations. The obtained set of linear equations is then inserted in the optimization problem. Depending on the integration step size, the number of new variables and constraints introduced to the original problem is drastically high which is a binding factor for the application of the proposed method in [15] for large-scale systems.

System spinning and operating reserves also suffer from high penetration level of intermittent and volatile generation. The reserve requirements for system primary and tertiary frequency responses are studied in [16]. The frequency deviation considered in [16] is based on static analysis, similar to governor load flow, and no information about the system dynamics is retrievable from the simulations. More specifically, the scope of [16] is to find the optimal reserve for the generation units to ensure enough primary and tertiary reserves for the system after a contingency. Optimal reserve requirements for a system with large amount of wind generation are calculated in [17]-[20] using stochastic optimization methods. Security-constrained unit commitment (SCUC) considering the volatile wind power generation is studied in [21] and stochastic techniques are applied to accurately model the wind generation behavior. It is also shown in [22] that stochastic optimization, compared to the deterministic methods, would reduce the system cost by 0.25% in the framework of unit commitment.

Although some research work has been carried out on system reserve requirements and unit commitment taking into account the probabilistic nature of wind speed, less attention has been paid to the system dynamic security with the presence of large wind generation. In fact, system reserves are usually activated to balance demand supply within 10 minutes and more. However, after a sudden disturbance, the system inertia in addition to the magnitude of the power imbalance are the main factors which determine the rate of decay of frequency and maximum system frequency drop. By increasing the penetration of wind generation into power systems, the number of conventional units which are committed to be online is reduced. This would bring up the problem of reduced inertial response which, in turn, leads to magnified frequency drops after contingencies. Reference [23] shows the possibility of endangering the system transient stability and/or frequency response in the presence of large wind power penetration. It is also shown that penetration level of wind farms could be limited by power system security constraints [23].

In this paper, an SCUC framework is proposed which addresses the problem of system reduced inertia and primary frequency control due to high level of wind generation integration. A simplified system frequency response model is first derived and used to find analytical representation of system minimum frequency in multi-machine systems. Then, an effective piecewise linearization (PWL) technique is employed here to linearize the nonlinear function representing the minimum system frequency, facilitating its integration in the SCUC problem. The optimization problem is formulated as a mixed-integer linear programming (MILP) problem and is solved using the Branch and Bound algorithm implemented in CPLEX [24].

The rest of the paper is organized as follows. In Section II, the basic concepts of frequency control in power systems and derivation of the simplified system frequency response are reviewed. A closed-form formula representing the maximum frequency drop for a multi-machine system is derived as well. Section III describes the formulation of the proposed SCUC framework with inertial response constraints. The results of applying the proposed method to two test systems are reported in Section IV. Section V concludes the results obtained in the present study.

II. Multi-Machine System Frequency Response Model

A. Power System Primary Frequency Control

The balance between the supplied and consumed power should be maintained during the power system operation to maintain synchronism. The smooth changes in the load is

met within day-ahead unit commitment and generators are scheduled to change their output power according to the load variation (load following). Based on this strategy for normal operation of power systems, the frequency is maintained within certain limits. However, if a sudden disturbance happens, particularly in terms of large generation loss, the system will undergo a transient, as shown in Fig. 1. The main focus of system frequency control is to help surviving from this transient period safely and rapidly.

There are four stages in a frequency transient phenomena. The time duration of these stages varies from system to system, depending on the governors control and system reserve. Right after the loss of generation, the frequency starts dropping with a certain rate of decay, which can be found by the swing equation of system equivalent single-machine representation [25]:

$$\Delta P_m - \Delta P_e = M\frac{d\Delta\omega}{dt} + D\Delta\omega \tag{1}$$

Assuming that there is no change in the mechanical power of prime movers in the very beginning of the incident ($\Delta P_m = 0$), and loads have no contribution in frequency response ($D = 0$), one will have:

$$\frac{d\Delta\omega}{dt} = -\frac{\Delta P_e}{M} \tag{2}$$

Therefore, the initial rate of decay of frequency mainly depends on the magnitude of the disturbance and the system equivalent inertia. The first stage in Fig. 1 (Δt_1), which is mainly governed by M and ΔP_e, is referred to as *system inertial response*. The duration of this stage is usually a few seconds.

After the first stage, the governors start to respond to the frequency drop, preventing it from further reduction. This stage, shown in Fig. 1 as Δt_2, is referred to as *primary frequency control*. The third stage in the frequency response begins when the governors cannot bring back the frequency to its original value (Δt_3 in Fig. 1). At this moment, the automatic generation control units participate in the frequency control and use their reserve to bring the frequency back. This stage is referred to as *secondary frequency control*. After this stage, further re-scheduling is performed to re-establish the system reserve for next possible disturbances. This stage is called *tertiary frequency control*. The main focus of the present work is to study the first and second stages, i.e. inertial and primary frequency responses.

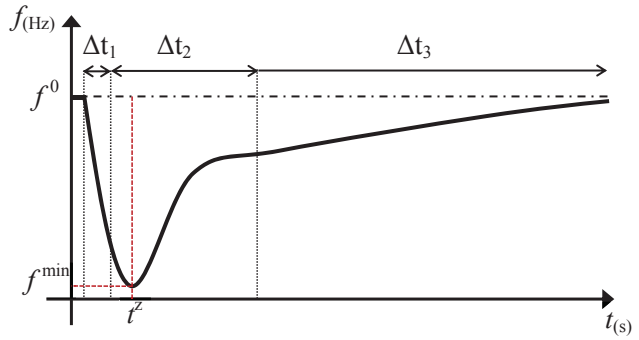

Fig. 1. Power system frequency transient after sudden loss of generation. Δt_1: Inertial Response; Δt_2: Primary Response; Δt_3: Secondary Response.

B. System Frequency Response Model

The simplest way to model the governor reactions is to use the single-machine equivalent model of the system, proposed by the authors in [1] as low-order system frequency response (SFR). This model is shown in Fig. 2. Apart from the simplicity of the low-order SFR model, there are a few shortcomings attached to it. First, it is not clarified how to calculate the parameters of the single-machine equivalent model based on the parameters of individual machines. Second, the contribution of each generator to the system frequency response is not clear. Therefore, if a particular machine is connected/disconnected, the impact on the system frequency response cannot be found.

Following the work presented in [1], the authors in [2] introduce a generalized SFR model capable of representing each governor contribution to the system frequency control. This model is depicted in Fig. 3. Although this model addresses the shortcomings of the previous model, it is still complicated and not clear how to find the closed-form time-domain response of the model based on each individual machine parameters.

C. Simplified Model for System Minimum Frequency Calculation

In this paper, we derive a simple, while still accurate enough, frequency response model for a multi-machine system based on the sensitivity of the frequency response to the governor parameters. To achieve this goal, the low-order model proposed in [1] is used to find the sensitivity of the frequency drop to the governor parameters. Table I gives the results of this analysis using a linear curve-fitting for finding the sensitivities. As can be seen, the system minimum frequency ($f^{\min}$) is less sensitive to the load damping factor (D) and governor time constant (T_R). Although the sensitivity of $f^{\min}$ to M is low, the sensitivity of the time at which $f^{\min}$ occurs, i.e. t^z, and the rate of decay of frequency are highly sensitive to M. Based on these results, we can assume identical values for T_R for all the system governors.

The transfer function of the system shown in Fig. 3 can be

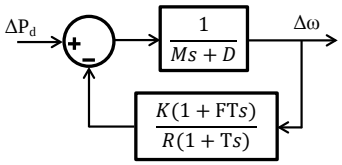

Fig. 2. First-order system frequency response model [1].

TABLE I
RESULTS OF THE ANALYSIS OF MINIMUM FREQUENCY SENSITIVITY TO THE SYSTEM PARAMETERS

Parameter (X)	K	T_R	H	F_H	D	R
Minimum	0.8	4	3	0.1	0	0.03
Maximum	1.2	11	9	0.35	2	0.08
Sensitivity ($\frac{\Delta f^{\min}}{\Delta X}$)	0.49	-0.01	0.03	1.35	0.05	-9.14

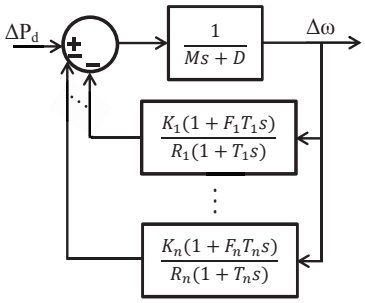

Fig. 3. General-order system frequency response model [2].

written as:

$$\frac{\Delta\omega}{\Delta P_d} = \frac{1}{(Ms+D) + \sum_{i\in N_g}\left[\frac{K_i}{R_i}\frac{1+sF_iT_i}{1+sT_i}\right]} \tag{3}$$

Assuming equal values for all the T_i as T, one can write:

$$\frac{\Delta\omega}{\Delta P_d} = \frac{1}{MT}\frac{1+sT}{s^2+2\xi w_n s + w_n^2} \tag{4}$$

where

$$w_n = \sqrt{\frac{1}{MT}\big(D+R_T\big)} \tag{5a}$$

$$\xi = \frac{1}{2}\frac{M+T(D+F_T)}{\sqrt{MT\big(D+R_T\big)}} \tag{5b}$$

$$F_T = \sum_{i\in N_g}\frac{K_iF_i}{R_i} \tag{5c}$$

$$R_T = \sum_{i\in N_g}\frac{K_i}{R_i} \tag{5d}$$

Assuming a step function for the disturbance, i.e. $\Delta P_d(s) = -\Delta P/s$, the time-domain response for $\Delta\omega$ can be derived as:

$$\Delta\omega(t) = -\frac{\Delta P}{MTw_n^2} - \frac{\Delta P}{Mw_r}e^{-\xi w_n t}\left(\sin(w_r t) - \frac{1}{w_n T}\sin(w_r t+\phi)\right) \tag{6}$$

in which

$$w_r = w_n\sqrt{1-\xi^2} \tag{7a}$$

$$\phi = \sin^{-1}(\sqrt{1-\xi^2}) \tag{7b}$$

In order to find the the extreme points of $\Delta\omega(t)$, we need to take its derivative:

$$\frac{d\Delta\omega}{dt} = 0 \longrightarrow t^z = \frac{1}{w_r}\tan^{-1}\left(\frac{w_r}{\xi w_n - 1/T}\right) \tag{8}$$

Substituting t^z into (6) and using a few features of trigonometric functions, one can find the value of the minimum frequency as:

$$\Delta\omega(t^z) = -\frac{\Delta P}{R_T+D}\left(1+e^{-\xi w_n t^z}\sqrt{\frac{T(R_T-F_T)}{M}}\right) \tag{9}$$

Assuming that the frequency right before the disturbance happens is f^0, the minimum frequency is calculated as:

$$f^{\min} = f^0 + f^0\Delta\omega(t^z) \tag{10}$$

The proposed model is referred to as multi-machine system frequency response (MM-SFR) model. The accuracy of the SFR model has been evaluated in [1] and [2]. Here, in order to support the results in [1]-[2], a time-domain simulation is done using the six-bus test system with three generators. System data are borrowed from [26] and generators dynamic data are given in Table II. For generators, the classical model is used and for governors, the simplified model given in the feedback of Fig. 2 is used. A sudden 10% increase in the total load occurs at $t = 0$. Figure 4 shows the speed of each generator and the average frequency obtained using MM-SFR model. As can be seen, the MM-SFR model follows the general behavior of speed curves by filtering out the inter-machine oscillations.

The minimum frequency function (10) is nonlinear and the goal is to include it in the SCUC formulation such that a mixed-integer nonlinear programming (MINLP) problem is avoided. This is due to the fact that the MINLP solvers usually impose high computational burden. In the next section, a PWL technique is utilized to represent (10) by means of linear functions and hence the SCUC problem would be a mixed-integer linear programming (MILP) problem.

D. PWL Technique for Linearizing the Minimum Frequency Function

Assume we have a nonlinear function, e.g. $f(X)$, of n variables, $X \in \mathbb{R}^n$. Assume also that f has local convexity within the interval of interest, e.g. $\underline{X} \le X \le \overline{X}$. One can represent $f(X)$ using a piecewise linear (PWL) function, with m pieces, defined by:

$$\tilde{f}(X) = \max_{1\le i\le m}\{c_i^t X + b_i\} \tag{11}$$

in which $c \in \mathbb{R}^n$ and $b \in \mathbb{R}$ are parameters to be determined. Suppose that we have k points of the function evaluation in the form of $([x_1, x_2, \ldots, x_n], f(X))$. The problem of fitting $\tilde{f}(X)$ to $f(X)$ over the range $\underline{X} \le X \le \overline{X}$ can be defined as:

$$\min_{\substack{c_j,b_j\\1\le j\le m}} \sum_{i=1}^{k}\Big(\max_{1\le j\le m}\{c_j^t X_i + b_j\} - f(X_i)\Big)^2 \tag{12}$$

A heuristic least-squares method is proposed in [27] to solve this problem. Observe that the "max" operator over a set of linear functions is convex, but cannot be handled by the linear programming solvers. Beside the method introduced in [27], there are commercial solvers which are able to solve this type of problems, e.g. CONOPT, KNITRO, LGO and IPOPT.

If the nonlinear function is the objective in a minimization problem, then substituting the original function with its PWL approximation leads to a "min-max" problem, which is easy to handle. This useful feature has been taken advantage of in PWL approximation of generators cost function in [28]. On the other hand, suppose that the nonlinear function has to be included in an optimization problem (e.g. SCUC) as a

TABLE II
SYSTEM DYNAMIC DATA FOR THE SIX-BUS TEST SYSTEM

Gen. No.	K	T_R	H	F_H	R	X'_d
1	0.9	8	7	0.15	0.04	0.061
2	0.95	7	5.5	0.35	0.03	0.120
3	0.98	9	3.5	0.25	0.05	0.181

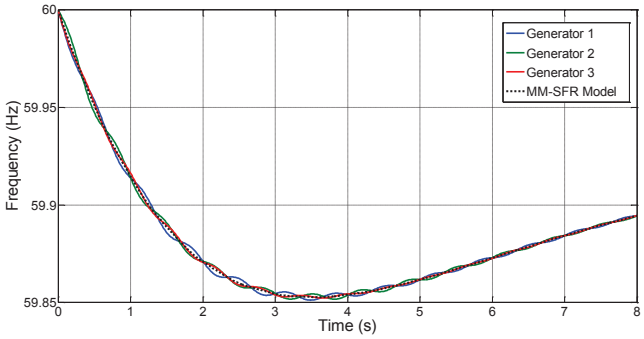

Fig. 4. System frequency response after a sudden 10% load increase in the six-bus system.

constraint. In this case, the approximation of the nonlinear function, i.e. $\tilde{f}(X)$, makes the problem non-smooth. One solution is to take the constraint to the objective function as a penalty term and establish a "min-max" problem. However, penalty terms would not necessarily satisfy the constraint and choosing a large penalizing value will cause numerical problems. For this reason, a technique is used here to partition the range introduced before, i.e. $\underline{X} \leq X \leq \overline{X}$, into corresponding section to each piece of the PWL approximation. This technique is discussed in [29]. It basically introduces $m-1$ new binary and continuous variables and $4*(m-1)$ new inequalities, all being linear. For instance, in order to represent the following constraint:

$$\max\{p, q\} \geq 0 \tag{13}$$

A new variable is introduced as $t = \max\{p, q\}$ and adding the following new constraints would relieve us from the "max" operator:

$$t \geq p \tag{14a}$$

$$t \geq q \tag{14b}$$

$$t \leq p + v\Omega \tag{14c}$$

$$t \leq q + (1 - v)\Omega \tag{14d}$$

Here, v is a binary variable and Ω is a sufficiently large positive scalar.

III. FORMULATION OF SCUC WITH FREQUENCY LIMIT CONSTRAINTS

The security-constrained unit commitment (SCUC) aims to find the best dispatch for the generators in a system to minimize the operation cost and, at the same time, meet the system operational constraints. As mentioned before, for all the credible contingencies across the system, the maximum frequency drop/increase should not exceed preset limits. In order to address this concern, the corresponding frequency response constraint based on generators governor responses (10) is included into the SCUC formulation as follows.

A. Mixed-Integer Formulation of SCUC

The objective in SCUC is to minimize the total operation cost over a period N_t defined by:

$$C_T = \sum_{i \in N_g} \sum_{h \in N_t} \left(b_{i,h} P_{i,h} + \text{SDn}_{i,h} + \text{SUp}_{i,h} \right) \tag{15}$$

where $b_{i,h}$ is the ith generator's bid for hour h; SDn and SUp are the shut-down and start-up costs, respectively. The problem is subject to the following operational constraints.

1) Active Power Flow Equations: Only the active power flows are considered (DC power flow). The reactive powers and voltage limits are not considered at this stage. For Bus i with a generation of P and a demand of P_d, one can write:

$$P_{i,h} - P_{d_{i,h}} = \sum_{j \in N_b} \bar{B}_{ij} \delta_j \tag{16}$$

2) Line Flow Limits: The power flow through each transmission line is limited by the system operational and security constraints. The DC power flow introduces the following constraints to the line flows:

$$-P_i^L \leq \sum_{j \in N_b} \bar{D}_{i,j} \delta_j \leq P_i^L \quad , \quad i \in N_l \tag{17}$$

3) Generation Limits: Each generation unit has a limit on the amount of power that can be generated by that unit. Also, instead of having a multiplication of the unit status (u) and its generation (P) which will introduce nonlinearity to the problem, the limits are multiplied by the unit status here. Therefore, if the unit is off-line, its output power is limited to zero and otherwise, its output power is limited to the actual limits, as follows:

$$P_i^{\min} u_{i,h} \leq P_{i,h} \leq P_i^{\max} u_{i,h} \tag{18}$$

4) Shutdown/Startup Costs: Beside the normal generation cost per MWh, each time that a unit needs to be shut down/start up, an extra cost will be imposed. If the status of the unit changes from one to zero, it means that unit is going off-line. Similarly, if the unit status is changing from zero to one, it means that unit is going on-line. Both cases can be covered by using the following set of equations:

$$\text{SUp}_{i,h} \geq (u_{i,h} - u_{i,h-1}) C_i^{\text{SUp}} \tag{19}$$

$$\text{SDn}_{i,h} \geq (u_{i,h-1} - u_{i,h}) C_i^{\text{SDn}} \tag{20}$$

$$\text{SUp}_{i,h} \geq 0 \tag{21}$$

$$\text{SDn}_{i,h} \geq 0 \tag{22}$$

It should be noted that if the status of a unit remains unchanged in two sequential time steps, (19)-(20) are the same as (21)-(22) and since the solver is minimizing the objective, the corresponding variable (SUp/SDn) will be zero.

5) Ramp Limits: Usually, a power turbine is not able to change its output power immediately. In order to meet this criterion, a cap has to be put on the maximum rate of change of the output power of each unit (R^{Up}). Also, if the unit is going from off-line to on-line status, there is a limit on the maximum power that can be delivered initially (P^{SUp}). Similar limits are also need to be met when the unit is being shut down. The following equations use the boolean logic to represent both the ramp rate and initial/final output power of generation units.

$$P_{i,h} - P_{i,h-1} \leq [u_{i,h} - u_{i,h-1}]P_i^{\text{SUp}} + u_{i,h-1}R_i^{\text{Up}} + [1 - u_{i,h}]P_i^{\max} \quad (23)$$

$$P_{i,h-1} - P_{i,h} \leq [u_{i,h-1} - u_{i,h}]P_i^{\text{SDn}} + u_{i,h}R_i^{\text{Dn}} + [1 - u_{i,h-1}]P_i^{\max} \quad (24)$$

6) Minimum Up/Down Time: Before a unit can be shut down, it has to stay on-line for a certain time after its initial connection to the gird. Likewise, when a unit is shut down, it needs to stay off-line for a certain time to be able to go on-line again. A linear representation of these constraints is proposed in [30] and is used here with slight modifications. The modifications are due to the infeasible cases produced by the formulation in [30]. For example, if the minimum up time for a unit is 5h and it has been up for 8h, then using the formula proposed in [30], G would be a negative quantity. The modified formulations are given in Appendix A.

7) Frequency Limit Constraints: The parameters representing the equivalent SFR model are calculated as:

$$\hat{F}_h = \sum_{i \in N_g} u_{i,h} \frac{K_i F_i}{R_i} \quad (25)$$

$$\hat{R}_h = \sum_{i \in N_g} u_{i,h} \frac{K_i}{R_i} \quad (26)$$

$$\hat{M}_h = \sum_{i \in N_g} 2u_{i,h} H_i \quad (27)$$

in which $\hat{F}_h$, $\hat{R}_h$ and $\hat{M}_h$ are dependent variables on $u_{i,h}$. Referring to the discussion in Section II-C, we can derive:

$$f_h^{\min} \leq f^0 + f^0 \Delta\omega_h(t_h^z) \quad (28)$$

The right-hand side of (28) is a function of three variables: $\hat{F}_h$, $\hat{R}_h$ and $\hat{M}_h$. The minimum and maximum values of these variables are obtained as:

$$\min_{i \in N_g} \{\frac{K_i F_i}{R_i}\} \leq \hat{F}_h \leq \sum_{i \in N_g} \frac{K_i F_i}{R_i}, \ \forall h \in N_t \quad (29a)$$

$$\min_{i \in N_g} \{\frac{K_i}{R_i}\} \leq \hat{R}_h \leq \sum_{i \in N_g} \frac{K_i}{R_i}, \ \forall h \in N_t \quad (29b)$$

$$\min_{i \in N_g} \{2H_i\} \leq \hat{M}_h \leq \sum_{i \in N_g} 2H_i, \ \forall h \in N_t \quad (29c)$$

Having these bounds on the variables and assuming a continuous relaxation, the PWL method introduced in Section II-D can be applied to replace the nonlinear constraint with its linearized equivalent set of constraints. By a few manipulation, (28) can be written as a nonlinear function being greater than or equal to 1, such that

$$\hat{R}_T \frac{f^0 - f^{\min}}{f^0 \Delta P} - e^{-\xi w_n t^z} \sqrt{\frac{T(\hat{R}_T - \hat{F}_T)}{\hat{M}}} \geq 1 \quad (30)$$

Let $g(\hat{R}_T, \hat{M}, \hat{F}_T)$ be the function on the left-hand side of (30). This function is point-wise convex within the range of variables used in this paper. If $g(\hat{R}_T, \hat{M}, \hat{F}_T)$ turns out to be point-wise concave in some regions, specially for small values of $\hat{M}$, then the convex PWL technique may not provide a tight approximation. In such cases, the variables domain is split into two regions over which the function is convex/concave. This can be done by introducing a binary variable and a few constraints to replace the disjunctive constraint [31]. Besides the introduced PWL technique here, there are other techniques that have no assumptions on the convexity of the original nonlinear function, e.g. [32]. The advantage of the PWL technique of [27] is that it optimally determines the intervals over which the linear segments are defined. This fact has also been acknowledged in [28].

The linearized equations representing g obtained using the PWL technique introduced in Section II-D are given in Appendix B. Figure 5 shows g and its approximation as a function of $\hat{F}_T$ and $\hat{R}_T$ for a fixed value of $\hat{M}$ and with $m = 4$.

IV. Simulation Results

In this section, two test systems are used to show the application of the proposed framework. Simulation results for two different cases are reported. In the first case, system frequency response is not considered, while in the second case it is considered by applying a 10% load increase, which is almost equivalent to a generation loss of the same magnitude. The significance of considering system frequency response is then revealed.

A sudden increase in the wind speed, known as wind gust, can also be considered as a contingency due to its unpredictability. Equivalently, a sudden loss of load represents this situation, which can be modeled by using a negative value for ΔP in (6). This is skipped here due to its similarity to the loss of generation case.

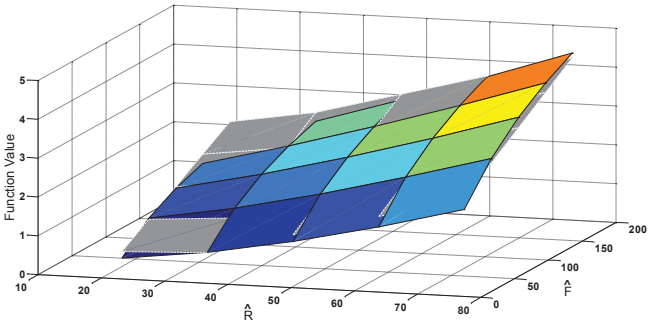

Fig. 5. Nonlinear function representing minimum frequency and its PWL approximation for $\hat{M} = 15$. The gray surface is the linear approximation and the colorful surface is the original function.

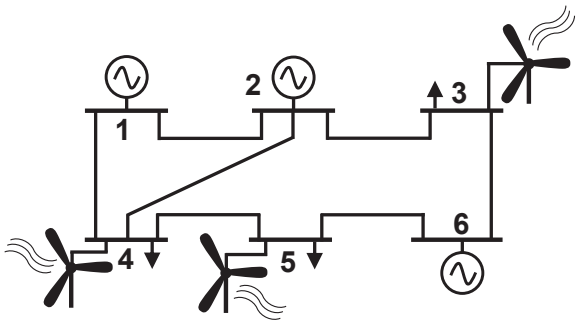

Fig. 6. The six-bus test system [26].

TABLE III
TOTAL DAY-AHEAD WIND GENERATION FORECAST DATA

Hour	1	2	3	4	5	6	7	8	9	10	11	12
P (MW)	10	12	15	25	49	51	32	45	56	50	43	40
Hour	13	14	15	16	17	18	19	20	21	22	23	24
P (MW)	52	50	45	41	32	10	5	12	24	21	16	14

A. The Six-bus Test System

The six-bus test system is shown in Fig. 6. The system data is given in [26] and the generators dynamic data are the same as the ones given in Table II. The load damping factor is assumed to be zero. At the peak hour, i.e. when the total load is 256 MW, the share of each load at buses 3, 4, and 5 is 80 MW, 110 MW and 66 MW, respectively. For the rest of the day, the total load is distributed between these buses with the same proportion. Total wind generation data is given in Table III. It is then distributed between the buses in a similar way as the total load.

In the first case, we use the SCUC without the frequency response constraints introduced in Section III-A7. The well-known MILP solver CPLEX 12.4 is used [24]. There are many advantages in using MILP solvers such as the capability of running multi-thread process which allows the utilization of multi-core CPU computers. The main algorithm is a Branch and Bound technique which also uses many other methods to enhance the performance of the solver.

The dispatch results are reported in Table IV. As can be seen, there are hours, i.e. 5 and 6, at which there is only one generator dispatched to be online. Figure 7 compares the frequency response of the system after a 10% load increase for three combinations of online generators reported in Table IV, i.e. $\{G_1\}$, $\{G_1, G_6\}$, and $\{G_1, G_2, G_6\}$. Having only one generator online, the frequency drops by almost 0.8 Hz, which might not be acceptable from the system operator point of view.

In the second case, the constraints given in Section III-A7 are added to the SCUC formulation. The limit on the maximum frequency drop is assumed to be 59.5 Hz. The new results are given in Table V. The total generation cost for the first and second cases are \$62330 and \$69639, respectively. With the new combination of the units in service, the maximum frequency drop occurs when only $\{G_1, G_6\}$ are online, which is 59.62 Hz.

TABLE IV
SCUC RESULTS WITHOUT FREQUENCY LIMIT CONSTRAINTS FOR THE SIX-BUS TEST SYSTEM.

Hour	1	2	3	4	5	6	7	8
G_1	140	140	133.7	129.7	106.1	109.5	131.4	122.6
G_2	-	-	-	-	-	-	-	-
G_6	25.2	13.2	10	-	-	-	10	10
Hour	9	10	11	12	13	14	15	16
G_1	120.8	131.4	140	140	140	140	140	140
G_2	-	-	-	-	-	-	-	-
G_6	10	25.6	45.6	56.1	50.2	53.6	63.9	74.8
Hour	17	18	19	20	21	22	23	24
G_1	140	140	140	140	140	140	128.3	140
G_2	-	10	10	-	-	-	-	-
G_6	84.0	86.7	91	85.4	73.3	71.7	51.7	41.6

TABLE V
SCUC RESULTS WITH FREQUENCY LIMIT CONSTRAINTS FOR THE SIX-BUS TEST SYSTEM

Hour	1	2	3	4	5	6	7	8
G_1	-	-	-	-	-	-	100	111.2
G_2	65.2	53.1	43.7	29.7	24.7	48.1	-	-
G_6	100	100	100	100	81.4	61.4	41.4	21.4
Hour	9	10	11	12	13	14	15	16
G_1	120.8	140	140	140	140	140	140	140
G_2	-	-	-	-	-	-	-	-
G_6	10	17	45.6	56.1	50.2	53.6	63.9	74.8
Hour	17	18	19	20	21	22	23	24
G_1	140	140	140	140	140	140	128.3	140
G_2	-	10	10	-	-	-	-	-
G_6	84	86.7	91	85.4	73.3	71.7	51.7	41.6

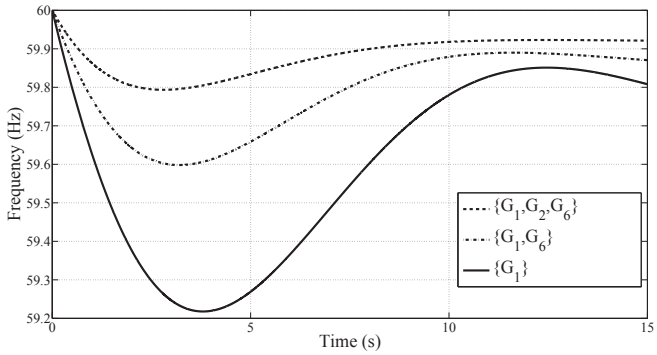

Fig. 7. System frequency response after 10% load increase for different combinations of online generators in the six-bus system.

B. The IEEE 118-bus Test System

The IEEE 118-bus test system consists of 54 generators, 186 lines, and 3733 MW peak load. The system data is given in [26] and for the generators and governors dynamic data, random values are selected within appropriate ranges. It is assumed that 10% of the load is supplied by wind generation, proportional to the total load at each hour. Two cases are simulated: the first case by ignoring the system frequency limit constraints and the second case by respecting them. In the first case, assuming a minimum allowable frequency of 59.5 Hz after a 10% sudden load increase, we have violation of the frequency limit in 16 different hours. This is shown in Table VI. Without the frequency limit constraint, the lowest value that the minimum frequency is dropped to is 59.14 Hz at Hour

TABLE VI
MINIMUM SYSTEM FREQUENCY AFTER A 10% SUPPLY-DEMAND DISTURBANCE FOR THE IEEE 118-BUS SYSTEM.

Hour	1	2	3	4	5	6
$f_1^{\min *}$	59.23	59.16	59.16	59.16	59.16	59.14
$f_2^{\min *}$	59.58	59.51	59.51	59.53	59.55	59.57
Hour	7	8	9	10	11	12
$f_1^{\min}$	59.26	59.33	59.48	59.54	59.53	59.53
$f_2^{\min}$	59.61	59.60	59.69	59.73	59.72	59.72
Hour	13	14	15	16	17	18
$f_1^{\min}$	59.53	59.44	59.40	59.40	59.53	59.53
$f_2^{\min}$	59.73	59.75	59.73	59.72	59.70	59.71
Hour	19	20	21	22	23	24
$f_1^{\min}$	59.51	59.51	59.47	59.32	59.25	59.22
$f_2^{\min}$	59.71	59.68	59.65	59.65	59.63	59.62

* $f_1^{\min}$ and $f_2^{\min}$ stand for the cases without and with a system frequency limit constraint, respectively.

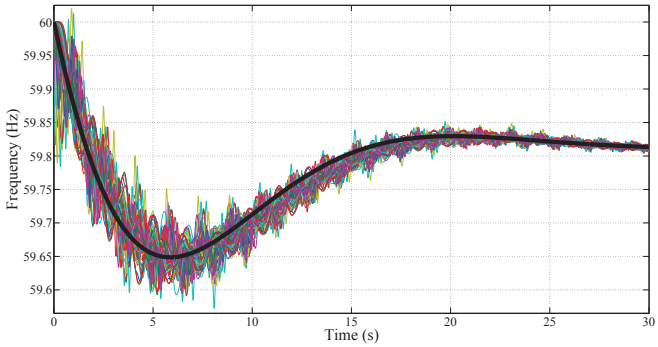

Fig. 8. System frequency response after 10% load increase for the IEEE 118-bus system at $h = 22$. The bold line is obtained using the SFR model.

6, while after adding the frequency limit, this value is increased to 59.51 Hz. By adding the frequency limit constraint to the SCUC problem, the system total generation cost is increased from \$487535 to \$496338, i.e. 1.8% increase. Despite the fact that the total generation cost is slightly increased, the frequency limit is respected at all the hours addressing one of the important system operators' concerns. The CPU time reported by CPLEX is about 28s for the first case and about 32s for the second case for providing the proven optimal solution.

In order to confirm that the frequency drop is above the threshold by the new generation schedule obtained using the SCUC with frequency limit constraints, a time-domain simulation is also conducted at $h = 22$. The results of this simulation along with the SFR simulation results are shown in Fig. 8. The SFR model shows the average variations in the frequency, neglecting the internal oscillations between synchronous machines.

It is important to mention that in addition to system frequency, increasing penetration of renewable resources may cause problems in system transient stability. This fact is studied in [23] in more detail. One of the causes for instability problem originates from the system reduced inertia. By applying the method in this paper, the overall system inertia is maintained and, therefore, this would, at least partially, resolve

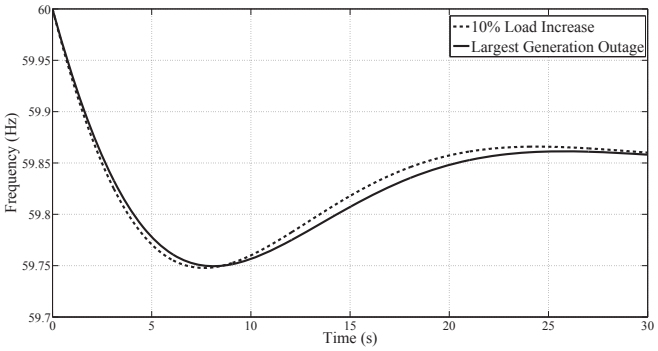

Fig. 9. A comparison of the system frequency response obtained after a 10% load increase and the loss of the largest unit for the IEEE 118-bus system at $h = 14$.

the mentioned problem of transient instability as well. This is beyond the scope of this paper and requires special studies.

C. Discussion

In this paper, the loss of the largest unit for the 118-bus system is simulated by a 10% sudden increase in the load. However, this will not lead to exactly the same results as losing a generation unit due to the following reason: losing a generator leads to the loss of its contribution in system inertial and governor responses. Therefore, it is worthwhile to show that the 10% load increase is fairly equivalent to (or even more severe than) the loss of the largest unit, as shown in Fig. 9. In order to show the equivalence of the loss of the largest generation to the 10% load increase, a scenario is considered assuming that the largest unit acts as base load generation and, therefore, the loss of the largest unit is modeled by considering ΔP being equal to the generation of the largest unit. The status of the largest unit is then forced to zero in the SFR model. As an example, this is done at $h = 14$ for the 118-bus system (considering the status of the units assigned by the SCUC) and the results are shown in Fig. 9. The difference between the maximum frequency drop in the two cases is about 0.01%, which is negligible. In general, the amount of load increase may be chosen based on the size of the largest unit in the system in order to more accurately simulate the loss of the largest unit by suddenly increasing the load as an equivalent.

In some real power systems, the largest unit (located in nuclear or coal power plants) serves as base load generation, i.e. the largest unit is known and its status does not depend on dispatch schedules. Therefore, one is able to accurately include its impact in the SFR model by removing the corresponding inertia and damping associated with the largest unit from the model. Alternatively, one may choose to always simulate the worst case scenario at all the hours which would lead to conservative results.

Another challenge for the systems with high level of wind generation is the sudden changes in wind speed, known as wind gust. This can also be modeled in the proposed framework. If the wind gust is predictable, the algorithm will take care of it. Otherwise, it can be modeled as a sudden power mismatch, similar to the loss of a generation unit, with a different sign for ΔP in the model shown in Fig.

3. In such instances, the system operator needs to ensure that there is sufficient reserve in the system to pick the power imbalance. The problem of determining the amount of spinning and non-spinning reserves required in the system considering the probabilistic and intermittent nature of wind generation has been previously studied in different references such as [17]-[20] and [33]. Also, sudden changes in wind generation output require rapid ramping (up/down) response from other generation units to retrieve the power balance as fast as possible. This is where the need for fast-responding energy resources is inevitable [34].

V. Conclusion

The problem of reduced system inertial and primary frequency responses due to high penetration level of renewable resources is addressed by means of an SCUC with system frequency limit constraints. By keeping enough synchronous generators in service at each hour, it is possible to respect the frequency limits. However, in order to increase the penetration level of the renewable resources, the system transient stability needs to be ensured as well. The main contributions of present study are summarized below:

- A closed-form formula representing the minimum frequency for a multi-machine system after a sudden power imbalance is derived.
- An effective piecewise linearization technique is utilized to linearize nonlinearities in the problem.
- An SCUC framework with system frequency limit constraints is proposed which can facilitate integrating higher penetration level of renewable resources.

In this study, it is assumed that the majority of generation is provided by thermal plants. As future work, for systems with considerable hydro generation, different transfer function has to be derived to appropriately model their governor response.

Appendix A
Minimum Up/Down Time

The constraints representing the minimum up/down times in [30] are as follows:

$$\sum_{m=1}^{T_i^{\text{Up}}-T_{i,0}^{\text{Up}}} [1-u_{i,m}] = 0 \quad (\text{if} \quad u_{i,0}=1 \text{ and } T_i^{\text{Up}} > T_{i,0}^{\text{Up}}) \tag{31a}$$

$$\sum_{m=k}^{k+T_i^{\text{Up}}-1} u_{i,m} \geq T_i^{\text{Up}}[u_{i,k}-u_{i,k-1}]$$
$$, k = G_i+1, \ldots, T-T_i^{\text{Up}}+1.$$
$$G_i = \begin{cases} u_{i,0}(T_i^{\text{Up}}-T_{i,0}^{\text{Up}}) & T_i^{\text{Up}} > T_{i,0}^{\text{Up}} \\ 0 & \text{otherwise} \end{cases} \tag{31b}$$

$$\sum_{m=k}^{T} [u_{i,m}-u_{i,k}+u_{i,k-1}] \geq 0, k = T-T_i^{\text{Up}}+2, \ldots, T. \tag{31c}$$

$$\sum_{m=1}^{T_i^{\text{Dn}}-T_{i,0}^{\text{Dn}}} u_{i,m} = 0 \quad (\text{if} \quad u_{i,0}=0 \text{ and } T_i^{\text{Dn}} > T_{i,0}^{\text{Dn}}) \tag{32a}$$

$$\sum_{m=k}^{k+T_i^{\text{Dn}}-1} [1-u_{i,m}] \geq T_i^{\text{Dn}}[u_{i,k-1}-u_{i,k}]$$
$$, k = W_i+1, \ldots, T-T_i^{\text{Dn}}+1.$$
$$W_i = \begin{cases} (1-u_{i,0})(T_i^{\text{Dn}}-T_{i,0}^{\text{Dn}}) & T_i^{\text{Dn}} > T_{i,0}^{\text{Dn}} \\ 0 & \text{otherwise} \end{cases} \tag{32b}$$

$$\sum_{m=k}^{T} [1-u_{i,m}-u_{i,k-1}+u_{i,k}] \geq 0$$
$$, k = T-T_i^{\text{Dn}}+2, \ldots, T. \tag{32c}$$

Appendix B
PWL Equations for (30)

The linearized equations representing the nonlinear function g in (30) are given here. The parameters used for numerical evaluation of g in (30) are $T=10$, $\Delta P=0.1$, $f^{\min}=59.5$, and $f^0=60$. Other parameters are generated using a Gaussian random number generator with the means (μ) and standard deviations (σ) given in Table VII.

Suppose that $\alpha_1=\hat{R}$, $\alpha_2=\hat{M}$, $\alpha_3=\hat{F}$. Then g can be represented as:

$$g(\alpha_1,\alpha_2,\alpha_3) = \max_{1\leq j\leq 4}\left\{\pi_j\right\} \tag{33}$$

where $\pi_j=\sum_{i=1}^{3}(a_{i,j}\alpha_i+a_{4,j})$. Parameters $a_{i,j}$ are obtained by solving the problem in (12). The resulting $a_{i,j}$ are:

$$\begin{bmatrix} 0.04319 & -0.05266 & -0.01601 & -0.05813 \\ 0.05329 & 0.02590 & -0.00420 & 0.00680 \\ 0.01299 & 0.01123 & -0.01744 & 0.01184 \\ -2.98348 & -0.00150 & -0.00054 & -0.00129 \end{bmatrix}$$

The recent PWL representation of g is then reformulated using the method explained in Section II-D (13)-(14), to avoid the max operator. Define $t_1=\max\{\pi_1,\pi_2\}$, $t_2=\max\{t_1,\pi_3\}$, $t_3=\max\{t_2,\pi_4\}$. With this splitting, t_3 is equivalent to g in (33). The following constraints are required:

$$\pi_1 \leq t_1 \leq \pi_1+v_1\Omega \tag{34a}$$
$$\pi_2 \leq t_1 \leq \pi_2+(1-v_1)\Omega \tag{34b}$$
$$t_1 \leq t_2 \leq t_1+v_2\Omega \tag{34c}$$
$$\pi_3 \leq t_2 \leq \pi_3+(1-v_2)\Omega \tag{34d}$$
$$t_2 \leq t_3 \leq t_2+v_3\Omega \tag{34e}$$
$$\pi_4 \leq t_3 \leq \pi_4+(1-v_3)\Omega \tag{34f}$$

Now, the nonlinear constraint in (30) is converted into $t_3 \geq 1$ with $t_3=g$ and (34). The three binary variables, i.e. v_1, v_2,

TABLE VII
Parameters for Gaussian Random Number Generator

Parameter	F_i	K_i	R_i	H_i
μ	0.25	1	0.04	4
σ	0.05	0.025	0.01	1.5

and v_3, have $2^3 = 8$ possible combinations. However, four out of these eight combinations lead to infeasible constraints which will be captured by the MILP solver.

REFERENCES

[1] P. M. Anderson and M. Mirheydar, "A low-order system frequency response model," *IEEE Trans. Power Syst.*, vol. 5, no. 3, pp. 720–729, Aug. 1990.

[2] D. L. H. Aik, "A general-order system frequency response model incorporating load shedding: analytic modeling and applications," *IEEE Trans. Power Syst.*, vol. 21, no. 2, pp. 709–717, May 2006.

[3] NAW. (2009, May) FERC study will use frequency response to assess integration. [Online]. Available: http://www.nawindpower.com.

[4] S. Sharma, S.-H. Huang, and N. D. R. Sarma, "System inertial frequency response estimation and impact of renewable resources in ERCOT interconnection," in *2011 IEEE PES General Meeting*, Jul. 2011, pp. 1–6.

[5] R. Pearmine, Y. H. Song, and A. Chebbo, "Influence of wind turbine behaviour on the primary frequency control of the British transmission grid," *IET Renew. Power Gen.*, vol. 1, no. 2, pp. 142–150, Jun. 2007.

[6] R. Doherty, A. Mullane, G. Nolan, D. J. Burke, A. Bryson, and M. O'Malley, "An assessment of the impact of wind generation on system frequency control," *IEEE Trans. Power Syst.*, vol. 25, no. 1, pp. 452–460, Feb. 2010.

[7] E. Vittal, "Static analysis of the maximum wind penetration level in Iowa and dynamic assessment of frequency response in wind turbine types," Master's thesis, Department of Electrical and Computer Engineering, Iowa State University, Ames, 2008.

[8] K. Antonakis, "Analysis of the maximum wind energy penetration in the Island of Crete," Master's thesis, Department of Electronic & Electrical Engineering, University of Strathclyde, Glasgow, Sep. 2005.

[9] P. Gardner, H. Snodin, A. Higgins, and S. McGoldrick, "The impacts of increased levels of wind penetration on the electricity systems of the republic of Ireland and Northern Ireland: Final report," Tech. Rep., Feb. 2003. [Online]. Available: http://www.cer.ie/cerdocs/cer03024.pdf

[10] D. Gautam, L. Goel, R. Ayyanar, V. Vittal, and T. Harbour, "Control strategy to mitigate the impact of reduced inertia due to doubly fed induction generators on large power systems," *IEEE Trans. Power Syst.*, vol. 26, no. 1, pp. 214–224, Feb. 2011.

[11] G. Abad, J. Lopez, M. Rodriguez, L. Marroyo, and G. Iwanski, *Doubly Fed Induction Machine: Modeling and Control for Wind Energy Generation*. John Wiley & Sons, Sep. 2011.

[12] H. Ahmadi and H. Ghasemi, "Probabilistic optimal power flow incorporating wind power using point estimate methods," in *2011 10th Int. Conf. Envir. Elect. Eng. (EEEIC)*, Rome, Italy, May 2011, pp. 1–5.

[13] R. Doherty, G. Lalor, and M. O'Malley, "Frequency control in competitive electricity market dispatch," *IEEE Trans. Power Syst.*, vol. 20, no. 3, pp. 1588–1596, Aug. 2005.

[14] M. Lotfalian, R. Schlueter, D. Idizior, P. Rusche, S. Tedeschi, L. Shu, and A. Yazdankhah, "Inertial, governor, and AGC/economic dispatch load flow simulations of loss of generation contingencies," *IEEE Trans. Power Appar. Syst.*, vol. PAS-104, no. 11, pp. 3020–3028, 1985.

[15] F. Ceja-Gomez, S. Qadri, and F. Galiana, "Under-frequency load shedding via integer programming," *IEEE Trans. Power Syst.*, vol. 27, no. 3, pp. 1387–1394, 2012.

[16] J. Restrepo and F. Galiana, "Unit commitment with primary frequency regulation constraints," *IEEE Trans. Power Syst.*, vol. 20, no. 4, pp. 1836–1842, 2005.

[17] L. Soder, "Reserve margin planning in a wind-hydro-thermal power system," *IEEE Trans. Power Syst.*, vol. 8, no. 2, pp. 564–571, May 1993.

[18] M. A. Ortega-Vazquez and D. S. Kirschen, "Estimating the spinning reserve requirements in systems with significant wind power generation penetration," *IEEE Trans. Power Syst.*, vol. 24, no. 1, pp. 114–124, Feb. 2009.

[19] J. M. Morales, A. J. Conejo, and J. Perez-Ruiz, "Economic valuation of reserves in power systems with high penetration of wind power," *IEEE Trans. Power Syst.*, vol. 24, no. 2, pp. 900–910, May 2009.

[20] T.-Y. Lee, "Optimal spinning reserve for a wind-thermal power system using EIPSO," *IEEE Trans. Power Syst.*, vol. 22, no. 4, pp. 1612–1621, Nov. 2007.

[21] J. Wang, M. Shahidehpour, and Z. Li, "Security-constrained unit commitment with volatile wind power generation," *IEEE Trans. Power Syst.*, vol. 23, no. 3, pp. 1319–1327, Aug. 2008.

[22] A. Tuohy, P. Meibom, E. Denny, and M. O'Malley, "Unit commitment for systems with significant wind penetration," *IEEE Trans. Power Syst.*, vol. 24, no. 2, pp. 592–601, May 2009.

[23] H. Ahmadi and H. Ghasemi, "Maximum penetration level of wind generation considering power system security limits," *IET Gener. Transm. Distrib.*, vol. 6, no. 11, pp. 1164–1170, May 2012.

[24] "IBM ILOG CPLEX optimization studio." [Online]. Available: http://www-01.ibm.com/software/integration/optimization/cplex-optimization-studio/

[25] P. Kundur and N. J. Balu, *Power System Stability and Control*. McGraw-Hill, Jan. 1998.

[26] Y. Fu, M. Shahidehpour, and Z. Li, "Security-constrained unit commitment with AC constraints*," *IEEE Trans. Power Syst.*, vol. 20, no. 3, pp. 1538–1550, Aug. 2005.

[27] A. Magnani and S. P. Boyd, "Convex piecewise-linear fitting," *Optimization and Engineering*, vol. 10, no. 1, pp. 1–17, 2009.

[28] H. Ahmadi, J. R. Marti, and A. Moshref, "Piecewise linear approximation of generators cost functions using max-affine functions," in *2013 IEEE PES General Meeting*, Jul. 2013, pp. 1–5.

[29] T. M. Burks and K. Sakallah, "Min-max linear programming and the timing analysis of digital circuits," in *, 1993 IEEE/ACM International Conference on Computer-Aided Design, 1993. ICCAD-93. Digest of Technical Papers*, Nov. 1993, pp. 152–155.

[30] M. Carrion and J. M. Arroyo, "A computationally efficient mixed-integer linear formulation for the thermal unit commitment problem," *IEEE Trans. Power Syst.*, vol. 21, no. 3, pp. 1371–1378, Aug. 2006.

[31] H. P. Williams, *Model building in mathematical programming*. John Wiley & Sons, 2013.

[32] R. Misener and C. A. Floudas, "Piecewise-linear approximations of multidimensional functions," *J. Optimization Theory and Applications*, vol. 145, no. 1, pp. 120–147, 2010.

[33] F. Bouffard and F. Galiana, "Stochastic security for operations planning with significant wind power generation," *IEEE Trans. Power Syst.*, vol. 23, no. 2, pp. 306–316, 2008.

[34] G. Delille, B. Francois, and G. Malarange, "Dynamic frequency control support by energy storage to reduce the impact of wind and solar generation on isolated power system's inertia," *IEEE Trans. Sust. Energy*, vol. 3, no. 4, pp. 931–939, 2012.

Hamed Ahmadi (S'11) received the B.Sc. and M.Sc. degrees in electrical engineering from the University of Tehran in 2009 and 2011, respectively. His research interests include power system stability and control, power system operation, smart grids and high voltage engineering. He is currently a Ph.D. candidate at the University of British Columbia, Vancouver, BC, Canada.

Hassan Ghasemi (S'01M'07SM'11) received the B.Sc. and M.Sc. degrees from the University of Tehran, Tehran, Iran, in 1999 and 2001, respectively, and the Ph.D. degree in electrical engineering from the University of Waterloo, Waterloo, ON, Canada, in 2006. He worked for the market and system operation division at the independent electricity system operator (IESO), Ontario, Canada, from 2006-2009. Currently, he is an Assistant Professor in the School of Electrical and Computer Engineering, University of Tehran. His main research interests are power system operation and control, energy systems, electricity markets and system identification applications to power systems.